

Evidence for a $Z_b^0(10610)$ in Dalitz analysis of $\Upsilon(5S) \rightarrow \Upsilon(nS)\pi^0\pi^0$

I. Adachi,¹³ K. Adamczyk,⁴⁵ H. Aihara,⁶⁹ K. Arinstein,² Y. Arita,³⁸ D. M. Asner,⁵¹
T. Aso,⁷³ V. Aulchenko,² T. Aushev,²⁴ T. Aziz,⁶⁴ A. M. Bakich,⁶³ Y. Ban,⁵³ E. Barberio,³⁷
M. Barrett,¹² A. Bay,³² I. Bedny,² M. Belhorn,⁵ K. Belous,²¹ V. Bhardwaj,⁴¹ B. Bhuyan,¹⁶
M. Bischofberger,⁴¹ S. Blyth,⁴³ A. Bondar,² G. Bonvicini,⁷⁵ A. Bozek,⁴⁵ M. Bračko,^{35, 25}
J. Brodzicka,⁴⁵ O. Brovchenko,²⁷ T. E. Browder,¹² M.-C. Chang,⁶ P. Chang,⁴⁴ Y. Chao,⁴⁴
V. Chekelian,³⁶ A. Chen,⁴² K.-F. Chen,⁴⁴ P. Chen,⁴⁴ B. G. Cheon,¹¹ K. Chilikin,²⁴
R. Chistov,²⁴ I.-S. Cho,⁷⁷ K. Cho,²⁸ K.-S. Choi,⁷⁷ S.-K. Choi,¹⁰ Y. Choi,⁶² J. Crnkovic,¹⁵
J. Dalseno,^{36, 65} M. Danilov,²⁴ J. Dingfelder,¹ Z. Doležal,³ Z. Drásal,³ A. Drutskoy,²⁴
W. Dungel,²⁰ D. Dutta,¹⁶ S. Eidelman,² D. Epifanov,² S. Esen,⁵ J. E. Fast,⁵¹ M. Feindt,²⁷
M. Fujikawa,⁴¹ V. Gaur,⁶⁴ N. Gabyshev,² A. Garmash,² Y. M. Goh,¹¹ B. Golob,^{33, 25}
M. Grosse Perdekamp,^{15, 57} H. Guo,⁵⁹ J. Haba,¹³ Y. L. Han,¹⁹ K. Hara,¹³ T. Hara,¹³
Y. Hasegawa,⁶¹ K. Hayasaka,³⁹ H. Hayashii,⁴¹ D. Heffernan,⁵⁰ T. Higuchi,¹³ Y. Horii,³⁹
Y. Hoshi,⁶⁷ K. Hoshina,⁷² W.-S. Hou,⁴⁴ Y. B. Hsiung,⁴⁴ H. J. Hyun,³¹ Y. Igarashi,¹³
T. Iijima,^{39, 38} M. Imamura,³⁸ K. Inami,³⁸ A. Ishikawa,⁶⁸ R. Itoh,¹³ M. Iwabuchi,⁷⁷
M. Iwasaki,⁶⁹ Y. Iwasaki,¹³ T. Iwashita,⁴¹ S. Iwata,⁷¹ I. Jaegle,¹² M. Jones,¹² T. Julius,³⁷
D. H. Kah,³¹ H. Kakuno,⁷¹ J. H. Kang,⁷⁷ P. Kapusta,⁴⁵ S. U. Kataoka,⁴⁰ N. Katayama,¹³
H. Kawai,⁴ T. Kawasaki,⁴⁷ H. Kichimi,¹³ C. Kiesling,³⁶ B. H. Kim,⁶⁰ H. J. Kim,³¹
H. O. Kim,³¹ J. B. Kim,²⁹ J. H. Kim,²⁸ K. T. Kim,²⁹ M. J. Kim,³¹ S. K. Kim,⁶⁰
Y. J. Kim,²⁸ K. Kinoshita,⁵ J. Klucar,²⁵ B. R. Ko,²⁹ N. Kobayashi,⁷⁰ S. Koblitz,³⁶
P. Kodyš,³ Y. Koga,³⁸ S. Korpar,^{35, 25} R. T. Kouzes,⁵¹ M. Kreps,²⁷ P. Križan,^{33, 25}
P. Krokovny,² B. Kronenbitter,²⁷ T. Kuhr,²⁷ R. Kumar,⁵² T. Kumita,⁷¹ E. Kurihara,⁴
Y. Kuroki,⁵⁰ A. Kuzmin,² P. Kvasnička,³ Y.-J. Kwon,⁷⁷ S.-H. Kyeong,⁷⁷ J. S. Lange,⁷
M. J. Lee,⁶⁰ S.-H. Lee,²⁹ M. Leitgab,^{15, 57} R. Leitner,³ J. Li,⁶⁰ X. Li,⁶⁰ Y. Li,⁷⁴ J. Libby,¹⁷
C.-L. Lim,⁷⁷ A. Limosani,³⁷ C. Liu,⁵⁹ Y. Liu,⁵ Z. Q. Liu,¹⁹ D. Liventsev,²⁴ R. Louvot,³²
J. MacNaughton,¹³ D. Marlow,⁵⁴ D. Matvienko,² A. Matyja,⁴⁵ S. McOnie,⁶³ Y. Mikami,⁶⁸
K. Miyabayashi,⁴¹ Y. Miyachi,⁷⁶ H. Miyata,⁴⁷ Y. Miyazaki,³⁸ R. Mizuk,²⁴ G. B. Mohanty,⁶⁴
D. Mohapatra,⁵¹ A. Moll,^{36, 65} T. Mori,³⁸ T. Müller,²⁷ N. Muramatsu,⁵⁵ R. Mussa,²³
T. Nagamine,⁶⁸ Y. Nagasaka,¹⁴ Y. Nakahama,⁶⁹ I. Nakamura,¹³ E. Nakano,⁴⁹ T. Nakano,⁵⁶
M. Nakao,¹³ H. Nakayama,¹³ H. Nakazawa,⁴² Z. Natkaniec,⁴⁵ M. Nayak,¹⁷ E. Nedelkovska,³⁶
K. Negishi,⁶⁸ K. Neichi,⁶⁷ S. Neubauer,²⁷ C. Ng,⁶⁹ M. Niiyama,³⁰ S. Nishida,¹³
K. Nishimura,¹² O. Nitoh,⁷² T. Nozaki,¹³ A. Ogawa,⁵⁷ S. Ogawa,⁶⁶ T. Ohshima,³⁸
S. Okuno,²⁶ S. L. Olsen,^{60, 12} Y. Onuki,⁶⁹ W. Ostrowicz,⁴⁵ H. Ozaki,¹³ P. Pakhlov,²⁴
G. Pakhlova,²⁴ H. Palka,⁴⁵ C. W. Park,⁶² H. Park,³¹ H. K. Park,³¹ K. S. Park,⁶²
L. S. Peak,⁶³ T. K. Pedlar,³⁴ T. Peng,⁵⁹ R. Pestotnik,²⁵ M. Peters,¹² M. Petrič,²⁵
L. E. Piilonen,⁷⁴ A. Poluektov,² M. Prim,²⁷ K. Prothmann,^{36, 65} B. Reisert,³⁶ M. Ritter,³⁶
M. Röhrken,²⁷ J. Rorie,¹² M. Rozanska,⁴⁵ S. Ryu,⁶⁰ H. Sahoo,¹² K. Sakai,¹³ Y. Sakai,¹³
S. Sandilya,⁶⁴ D. Santel,⁵ L. Santelj,²⁵ T. Sanuki,⁶⁸ N. Sasao,³⁰ Y. Sato,⁶⁸ O. Schneider,³²
P. Schönmeier,⁶⁸ C. Schwanda,²⁰ A. J. Schwartz,⁵ R. Seidl,⁵⁷ A. Sekiya,⁴¹ K. Senyo,⁷⁶
O. Seon,³⁸ M. E. Sevier,³⁷ L. Shang,¹⁹ M. Shapkin,²¹ V. Shebalin,² C. P. Shen,³⁸
T.-A. Shibata,⁷⁰ H. Shibuya,⁶⁶ S. Shinomiya,⁵⁰ J.-G. Shiu,⁴⁴ B. Shwartz,² A. Sibidanov,⁶³
F. Simon,^{36, 65} J. B. Singh,⁵² R. Sinha,²² P. Smerkol,²⁵ Y.-S. Sohn,⁷⁷ A. Sokolov,²¹

E. Solovieva,²⁴ S. Stanič,⁴⁸ M. Starič,²⁵ J. Stypula,⁴⁵ S. Sugihara,⁶⁹ A. Sugiyama,⁵⁸
M. Sumihama,⁸ K. Sumisawa,¹³ T. Sumiyoshi,⁷¹ K. Suzuki,³⁸ S. Suzuki,⁵⁸ S. Y. Suzuki,¹³
H. Takeichi,³⁸ U. Tamponi,²³ M. Tanaka,¹³ S. Tanaka,¹³ K. Tanida,⁶⁰ N. Taniguchi,¹³
G. Tatishvili,⁵¹ G. N. Taylor,³⁷ Y. Teramoto,⁴⁹ F. Thorne,²⁰ I. Tikhomirov,²⁴ K. Trabelsi,¹³
Y. F. Tse,³⁷ T. Tsuboyama,¹³ M. Uchida,⁷⁰ T. Uchida,¹³ Y. Uchida,⁹ S. Uehara,¹³
K. Ueno,⁴⁴ T. Uglov,²⁴ Y. Unno,¹¹ S. Uno,¹³ P. Urquijo,¹ Y. Ushiroda,¹³ Y. Usov,²
S. E. Vahsen,¹² P. Vanhoefer,³⁶ G. Varner,¹² K. E. Varvell,⁶³ K. Vervink,³² A. Vinokurova,²
V. Vorobyev,² A. Vossen,¹⁸ C. H. Wang,⁴³ J. Wang,⁵³ M.-Z. Wang,⁴⁴ P. Wang,¹⁹
X. L. Wang,¹⁹ M. Watanabe,⁴⁷ Y. Watanabe,²⁶ R. Wedd,³⁷ E. White,⁵ J. Wicht,¹³
L. Widhalm,²⁰ J. Wiechczynski,⁴⁵ K. M. Williams,⁷⁴ E. Won,²⁹ B. D. Yabsley,⁶³
H. Yamamoto,⁶⁸ J. Yamaoka,¹² Y. Yamashita,⁴⁶ M. Yamauchi,¹³ C. Z. Yuan,¹⁹ Y. Yusa,⁴⁷
D. Zander,²⁷ C. C. Zhang,¹⁹ L. M. Zhang,⁵⁹ Z. P. Zhang,⁵⁹ L. Zhao,⁵⁹ V. Zhilich,²
P. Zhou,⁷⁵ V. Zhulanov,² T. Zivko,²⁵ A. Zupanc,²⁷ N. Zwahlen,³² and O. Zyukova²

(The Belle Collaboration)

¹*University of Bonn, Bonn*

²*Budker Institute of Nuclear Physics SB RAS and
Novosibirsk State University, Novosibirsk 630090*

³*Faculty of Mathematics and Physics, Charles University, Prague*

⁴*Chiba University, Chiba*

⁵*University of Cincinnati, Cincinnati, Ohio 45221*

⁶*Department of Physics, Fu Jen Catholic University, Taipei*

⁷*Justus-Liebig-Universität Gießen, Gießen*

⁸*Gifu University, Gifu*

⁹*The Graduate University for Advanced Studies, Hayama*

¹⁰*Gyeongang National University, Chinju*

¹¹*Hanyang University, Seoul*

¹²*University of Hawaii, Honolulu, Hawaii 96822*

¹³*High Energy Accelerator Research Organization (KEK), Tsukuba*

¹⁴*Hiroshima Institute of Technology, Hiroshima*

¹⁵*University of Illinois at Urbana-Champaign, Urbana, Illinois 61801*

¹⁶*Indian Institute of Technology Guwahati, Guwahati*

¹⁷*Indian Institute of Technology Madras, Madras*

¹⁸*Indiana University, Bloomington, Indiana 47408*

¹⁹*Institute of High Energy Physics,*

Chinese Academy of Sciences, Beijing

²⁰*Institute of High Energy Physics, Vienna*

²¹*Institute of High Energy Physics, Protvino*

²²*Institute of Mathematical Sciences, Chennai*

²³*INFN - Sezione di Torino, Torino*

²⁴*Institute for Theoretical and Experimental Physics, Moscow*

²⁵*J. Stefan Institute, Ljubljana*

²⁶*Kanagawa University, Yokohama*

²⁷*Institut für Experimentelle Kernphysik,*

Karlsruher Institut für Technologie, Karlsruhe

²⁸*Korea Institute of Science and Technology Information, Daejeon*

- ²⁹*Korea University, Seoul*
- ³⁰*Kyoto University, Kyoto*
- ³¹*Kyungpook National University, Taegu*
- ³²*École Polytechnique Fédérale de Lausanne (EPFL), Lausanne*
- ³³*Faculty of Mathematics and Physics, University of Ljubljana, Ljubljana*
- ³⁴*Luther College, Decorah, Iowa 52101*
- ³⁵*University of Maribor, Maribor*
- ³⁶*Max-Planck-Institut für Physik, München*
- ³⁷*University of Melbourne, School of Physics, Victoria 3010*
- ³⁸*Graduate School of Science, Nagoya University, Nagoya*
- ³⁹*Kobayashi-Maskawa Institute, Nagoya University, Nagoya*
- ⁴⁰*Nara University of Education, Nara*
- ⁴¹*Nara Women's University, Nara*
- ⁴²*National Central University, Chung-li*
- ⁴³*National United University, Miao Li*
- ⁴⁴*Department of Physics, National Taiwan University, Taipei*
- ⁴⁵*H. Niewodniczanski Institute of Nuclear Physics, Krakow*
- ⁴⁶*Nippon Dental University, Niigata*
- ⁴⁷*Niigata University, Niigata*
- ⁴⁸*University of Nova Gorica, Nova Gorica*
- ⁴⁹*Osaka City University, Osaka*
- ⁵⁰*Osaka University, Osaka*
- ⁵¹*Pacific Northwest National Laboratory, Richland, Washington 99352*
- ⁵²*Panjab University, Chandigarh*
- ⁵³*Peking University, Beijing*
- ⁵⁴*Princeton University, Princeton, New Jersey 08544*
- ⁵⁵*Research Center for Electron Photon Science, Tohoku University, Sendai*
- ⁵⁶*Research Center for Nuclear Physics, Osaka University, Osaka*
- ⁵⁷*RIKEN BNL Research Center, Upton, New York 11973*
- ⁵⁸*Saga University, Saga*
- ⁵⁹*University of Science and Technology of China, Hefei*
- ⁶⁰*Seoul National University, Seoul*
- ⁶¹*Shinshu University, Nagano*
- ⁶²*Sungkyunkwan University, Suwon*
- ⁶³*School of Physics, University of Sydney, NSW 2006*
- ⁶⁴*Tata Institute of Fundamental Research, Mumbai*
- ⁶⁵*Excellence Cluster Universe, Technische Universität München, Garching*
- ⁶⁶*Toho University, Funabashi*
- ⁶⁷*Tohoku Gakuin University, Tagajo*
- ⁶⁸*Tohoku University, Sendai*
- ⁶⁹*Department of Physics, University of Tokyo, Tokyo*
- ⁷⁰*Tokyo Institute of Technology, Tokyo*
- ⁷¹*Tokyo Metropolitan University, Tokyo*
- ⁷²*Tokyo University of Agriculture and Technology, Tokyo*
- ⁷³*Toyama National College of Maritime Technology, Toyama*
- ⁷⁴*CNP, Virginia Polytechnic Institute and State University, Blacksburg, Virginia 24061*
- ⁷⁵*Wayne State University, Detroit, Michigan 48202*

⁷⁶*Yamagata University, Yamagata*
⁷⁷*Yonsei University, Seoul*

Abstract

We report the first observation of $\Upsilon(5S) \rightarrow \Upsilon(1,2S)\pi^0\pi^0$ decays. Evidence for the $Z_b^0(10610)$ with 4.9σ significance is found in a Dalitz plot analysis of $\Upsilon(5S) \rightarrow \Upsilon(2S)\pi^0\pi^0$ decays. The results are obtained with a 121.4fb^{-1} data sample collected with the Belle detector at the $\Upsilon(5S)$ resonance at the KEKB asymmetric-energy e^+e^- collider.

PACS numbers: 14.40.Pq, 13.25.Gv, 12.39.Pn

INTRODUCTION

Recently the Belle Collaboration reported the observation of two narrow structures in $\pi^\pm \Upsilon(nS)$ invariant mass in the $\Upsilon(5S) \rightarrow \Upsilon(nS)\pi^+\pi^-$ decays ($n = 1, 2, 3$) [1]. The measured masses and widths of the two structures are $M_1 = 10607.2 \pm 2.0$ MeV/ c^2 , $\Gamma_1 = 18.4 \pm 2.4$ MeV and $M_2 = 10652.2 \pm 1.5$ MeV/ c^2 , $\Gamma_2 = 11.5 \pm 2.2$ MeV, respectively. Angular analysis suggests that these states have $I^G(J^P) = 1^+(1^+)$ quantum numbers [2]. The measured masses are a few MeV/ c^2 above the thresholds for the open beauty channels $B^*\bar{B}$ (10604.6 MeV/ c^2) and $B^*\bar{B}^*$ (10604.6 MeV/ c^2) suggesting a “molecular” nature for these states, which is consistent with many of their observed properties [3]. This observation motivates us to search for a neutral partner of these states in the resonant substructure of $\Upsilon(5S) \rightarrow \Upsilon(nS)\pi^0\pi^0$ decays.

SELECTION CRITERIA

We use a 121.4 ± 1.9 fb $^{-1}$ data sample collected on the peak of the $\Upsilon(5S)$ resonance with the Belle detector [4] at the KEKB asymmetric energy e^+e^- collider [5]. The Belle detector is a large-solid-angle magnetic spectrometer that consists of a silicon vertex detector, a central drift chamber, an array of aerogel threshold Cherenkov counters, a barrel-like arrangement of time-of-flight scintillation counters, and an electromagnetic calorimeter comprised of CsI(Tl) crystals located inside a superconducting solenoid that provides a 1.5 T magnetic field. An iron flux-return located outside the coil is instrumented to detect K_L^0 mesons and to identify muons. The detector is described in detail elsewhere [4].

$\Upsilon(5S)$ candidates are formed from $\Upsilon(nS)\pi^0\pi^0$ ($n = 1, 2$) combination. We reconstruct $\Upsilon(nS)$ candidates from pairs of leptons (e^+e^- and $\mu^+\mu^-$) with invariant mass in the range from 8 to 11 GeV/ c^2 . An additional decay channel is used for the $\Upsilon(2S)$: $\Upsilon(2S) \rightarrow \Upsilon(1S)[l^+l^-]\pi^+\pi^-$. Charged tracks are required to have transverse momentum, $p_t >$, greater than 50 MeV/ c . We also impose a requirement on the impact parameters: $dr < 0.3$ cm and $|dz| < 2.0$ cm, where dr and dz are the impact parameters in the r - ϕ and longitudinal directions, respectively. Muon and electron candidates are required to be positively identified. No requirement on the particle identification is used for the pions. Candidate π^0 mesons are selected from pairs of photons with an invariant mass within 15 MeV/ c^2 of the nominal π^0 mass. Energy greater than 50 (75) MeV is required for each photon in the barrel (endcap). We use the quality of the π^0 mass-constrained fits to suppress the background; the sum of $\chi^2(\pi_1^0) + \chi^2(\pi_2^0)$ is required to be less than 20 (10) for the $\Upsilon(nS) \rightarrow \mu^+\mu^-$, $\Upsilon(1S)\pi^+\pi^-$ ($\Upsilon(nS) \rightarrow e^+e^-$).

We use the energy difference, $\Delta E = E_{\text{cand}} - E_{\text{CM}}$, and momentum P to suppress background, where E_{cand} and P are the energy and momentum of the reconstructed $\Upsilon(5S)$ candidate in the center-of-mass (c.m.) frame, and E_{CM} is the c.m. energy of the two beams. $\Upsilon(5S)$ candidates are required to satisfy the requirements $-0.2 < \Delta E < 0.14$ GeV and $P < 0.2$ GeV/ c . The large potential background from QED processes such as $e^+e^- \rightarrow l^+l^-(n)\gamma$ is suppressed using the missing mass associated with the l^+l^- system, $M_{\text{miss}}(l^+l^-)$, calculated as $M_{\text{miss}}(l^+l^-) = \sqrt{(E_{\text{CM}} - E_{l^+l^-})^2 - P_{l^+l^-}^2}$, where $E_{l^+l^-}$ and $P_{l^+l^-}$ are the energy and momentum of the l^+l^- system measured in the c.m. frame. We require $M_{\text{miss}}(l^+l^-) > 0.15$ (0.30) GeV/ c^2 for the $\Upsilon(nS) \rightarrow \mu^+\mu^-$ (e^+e^-). We select the candidate with the smallest $\chi^2(\pi_1^0) + \chi^2(\pi_2^0)$ in the rare cases (1-2%) in which there is more than one candidate in the event.

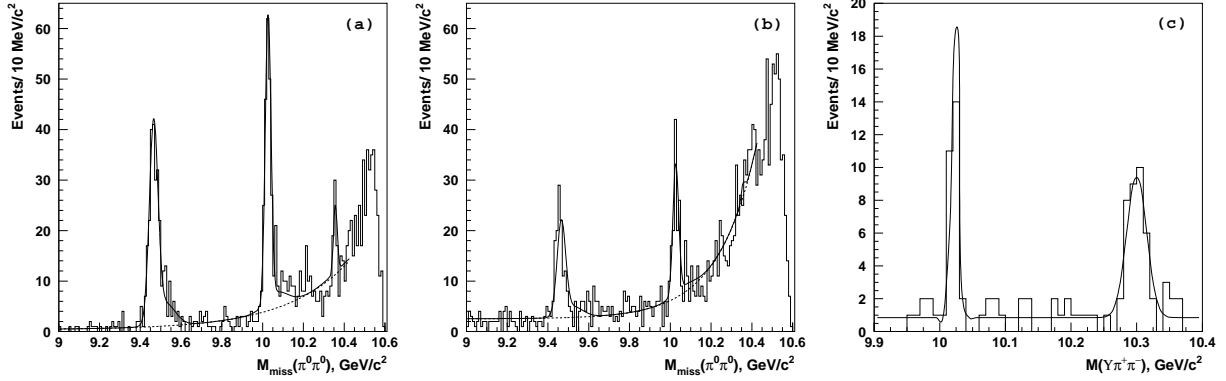


FIG. 1: The $\pi^0\pi^0$ missing mass distribution for $\Upsilon(nS)\pi^0\pi^0$, (a) $\Upsilon(nS) \rightarrow \mu^+\mu^-$ and (b) $\Upsilon(nS) \rightarrow e^+e^-$ candidates. The $M(\Upsilon(1S)\pi^+\pi^-)$ distribution for $\Upsilon(2S) \rightarrow \Upsilon(1S)\pi^+\pi^-$ candidates is shown in (c). Histograms represent the data. The solid curves show the fit result while the dashed curves correspond to the background contributions.

$\Upsilon(5S) \rightarrow \Upsilon(nS)[l^+l^-]\pi^0\pi^0$ candidates are identified via the missing mass recoiling against the $\pi^0\pi^0$ system, $M_{\text{miss}}(\pi^0\pi^0)$. Figures 1 (a) and 1 (b) show the $M_{\text{miss}}(\pi^0\pi^0)$ distributions for $\Upsilon(5S) \rightarrow \Upsilon(nS)[l^+l^-]\pi^0\pi^0$ candidates. We fit these distributions to extract the $\Upsilon(nS)$ signal yield. The signal probability density function (PDF) is described by a sum of two Gaussians for each $\Upsilon(nS)$ resonance with parameters fixed from the signal Monte Carlo (MC) sample. The background PDF is parameterized by the sum of constant and exponential functions.

For $\Upsilon(5S) \rightarrow \Upsilon(2S)[\Upsilon(1S)\pi^+\pi^-]\pi^0\pi^0$ decays, $\Upsilon(1S)$ candidates are selected from l^+l^- pairs with invariant mass within $150 \text{ MeV}/c^2$ of the nominal $\Upsilon(1S)$ mass. A mass-constrained fit is used for $\Upsilon(1S)$ candidates to improve the momentum resolution. We apply the same requirements on ΔE and P described above for reconstructed $\Upsilon(5S)$ candidate. We use the invariant mass of $\Upsilon(1S)\pi^+\pi^-$ to select the signal candidates. Figure 1 (c) shows the $M(\Upsilon(1S)\pi^+\pi^-)$ distribution for the $[\Upsilon(1S)\pi^+\pi^-]\pi^0\pi^0$ events. We fit this distribution to extract the $\Upsilon(2S)[\Upsilon(1S)\pi^+\pi^-]$ signal yield. The signal PDF is described by a Gaussian function with parameters fixed from signal MC. The background PDF is described by a constant. The cross-feed from the decay $\Upsilon(5S) \rightarrow \Upsilon(2S)[\Upsilon(1S)\pi^0\pi^0]\pi^+\pi^-$ contributes as a broad peak around $10.3 \text{ GeV}/c^2$. Its contribution is parameterized by a Gaussian function.

Table I summarizes the definition of the signal region, signal yield, MC efficiency, measured branching fraction (only the statistical uncertainty is shown), number of selected events and purity. The reconstruction efficiency is obtained using MC with the $\Upsilon(nS)\pi^0\pi^0$ system distributed uniformly over three-body phase space. The branching fraction is calculated by $\mathcal{B} = \frac{N_{\text{sig}}}{\epsilon \mathcal{L} \sigma(e^+e^- \rightarrow \Upsilon(5S))}$, where N_{sig} is number of signal events, ϵ is reconstruction efficiency, \mathcal{L} is integrated luminosity. We use the value of $\sigma(e^+e^- \rightarrow \Upsilon(5S)) = 0.340 \pm 0.016 \text{ nb}$ obtained with 121.4 fb^{-1} data.

The main sources of systematic uncertainty in the branching fraction measurement are: uncertainties in the signal and background PDFs used in the fit mainly due to data/MC width differences: 5%; uncertainty in the $e^+e^- \rightarrow \Upsilon(5S)$ cross section: 5%; $\mathcal{B}(\Upsilon(nS) \rightarrow l^+l^-)$: 2% and 9% for the $\Upsilon(1S)$ and $\Upsilon(2S)$ [7]; luminosity: 1.5%; π^0 reconstruction: 5%; muon identification: 1%; electron identification: 3%; tracking: 0.7%. The total systematic errors are 9% for $\Upsilon(1S)\pi^0\pi^0$ and 13% for $\Upsilon(2S)\pi^0\pi^0$. We calculate the weighted average of $\mathcal{B}(\Upsilon(5S) \rightarrow \Upsilon(nS)\pi^0\pi^0)$ in the various $\Upsilon(nS)$ decay channels and obtain $\mathcal{B}(\Upsilon(5S) \rightarrow$

TABLE I: Definition of the signal region, signal yield, MC efficiency, measured branching fraction, number of selected events and purity.

Final state	Signal region, GeV/c^2	Signal yield	ϵ , %	\mathcal{B} , 10^{-3}	Events	Purity
$\Upsilon(1S) \rightarrow \mu^+\mu^-$	$9.41 < M_{\text{miss}}(\pi^0\pi^0) < 9.53$	261 ± 15	11.2	2.28 ± 0.13	247	0.95
$\Upsilon(1S) \rightarrow e^+e^-$	$9.41 < M_{\text{miss}}(\pi^0\pi^0) < 9.53$	123 ± 13	5.61	2.15 ± 0.23	140	0.78
$\Upsilon(2S) \rightarrow \mu^+\mu^-$	$9.99 < M_{\text{miss}}(\pi^0\pi^0) < 10.07$	241 ± 18	8.04	3.77 ± 0.28	253	0.87
$\Upsilon(2S) \rightarrow e^+e^-$	$9.99 < M_{\text{miss}}(\pi^0\pi^0) < 10.07$	108 ± 13	3.58	3.84 ± 0.46	151	0.66
$\Upsilon(2S) \rightarrow \Upsilon(1S)\pi^+\pi^-$	$10.00 < M(\Upsilon\pi^+\pi^-) < 10.05$	24 ± 5	2.27	2.85 ± 0.60	28	0.86

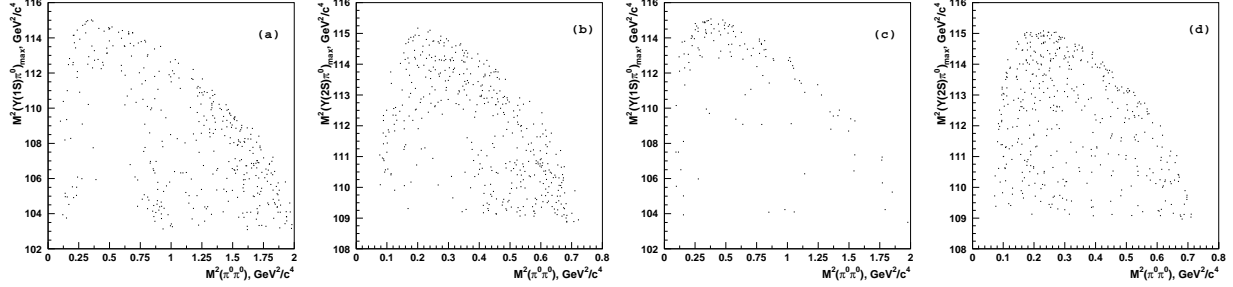


FIG. 2: Dalitz plots for selected (a) $\Upsilon(1S)\pi^0\pi^0$, (b) $\Upsilon(2S)\pi^0\pi^0$ candidates. Dalitz plots for events in the (c) $\Upsilon(1S)\pi^0\pi^0$, (d) $\Upsilon(2S)\pi^0\pi^0$ sidebands.

$\Upsilon(1S)\pi^0\pi^0 = (2.25 \pm 0.11 \pm 0.20) \times 10^{-3}$ and $\mathcal{B}(\Upsilon(5S) \rightarrow \Upsilon(2S)\pi^0\pi^0) = (3.66 \pm 0.22 \pm 0.48) \times 10^{-3}$. These are approximately one half of the corresponding values of $\mathcal{B}(\Upsilon(5S) \rightarrow \Upsilon(nS)\pi^+\pi^-)$ [9], consistent with expectations from isospin.

DALITZ ANALYSIS

We define the following sideband regions for the study of background: for the $\Upsilon(1S)\pi^0\pi^0$ final state : $9.20 \text{ GeV}/c^2 < M_{\text{miss}}(\pi^0\pi^0) < 9.35 \text{ GeV}/c^2$ and $9.60 \text{ GeV}/c^2 < M_{\text{miss}}(\pi^0\pi^0) < 9.75 \text{ GeV}/c^2$; and for the $\Upsilon(2S)\pi^0\pi^0$ final state: $9.80 \text{ GeV}/c^2 < M_{\text{miss}}(\pi^0\pi^0) < 9.95 \text{ GeV}/c^2$ and $10.15 \text{ GeV}/c^2 < M_{\text{miss}}(\pi^0\pi^0) < 10.30 \text{ GeV}/c^2$. Figure 2 shows the Dalitz plot distributions for the selected $\Upsilon(5S) \rightarrow \Upsilon(nS)\pi^0\pi^0$ candidates from the signal region and sidebands. Before analyzing Dalitz distributions for events in the signal region, we determine the PDF for background. Samples of background events are selected in $\Upsilon(nS)$ mass sidebands and then refitted to the nominal mass of the corresponding $\Upsilon(nS)$ state to match the phase space boundaries. We parameterize the background PDF by the following function:

$$1 + p_1 \exp(-q_1 s_3 + p_2 \exp(-q_2(s_{\text{min}} - a_2))), \quad (1)$$

where p_1 , p_2 , q_1 and q_2 are fit parameters. Here $s_3 = M^2(\pi^0\pi^0)$ and $s_{\text{min}} = \text{Min}(s_1, s_2)$, $s_{1,2} = M^2(\Upsilon(nS)\pi_{1,2}^0)$. The kinematical limit a_2 is 92 and 103 GeV^2/c^4 for the $\Upsilon(1S)$ and $\Upsilon(2S)$, respectively. Variation of the reconstruction efficiency over the Dalitz plot is determined using a large sample of MC with a uniform phase space distribution. We use the following function to parameterize efficiency variations:

$$\epsilon = 1 + c\{1 - e^{-(s_3 - a_0)/b_0}\}\{1 - e^{-(a_1 - s_{\text{max}})/b_1}\}, \quad (2)$$

where c , b_0 and b_1 are fit parameters. Here $s_{\max} = \text{Max}(s_1, s_2)$. The parameters a_0 and a_1 are defined as $a_0 = 4m_{\pi^0}^2$, $a_1 = (m_{\Upsilon(5S)} - m_{\pi^0})^2$.

The amplitude analysis of three-body $\Upsilon(5S) \rightarrow \Upsilon(nS)\pi^0\pi^0$ decays uses an unbinned maximum likelihood fit. We describe the three-body signal amplitude as a sum of quasi-two-body amplitudes:

$$M(s_1, s_2) = A_{Z_1} + A_{Z_2} + A_{f_0} + A_{f_2} + A_{\text{nr}} , \quad (3)$$

where A_{Z_1} and A_{Z_2} are amplitudes for contributions from the $Z_b^0(10610)$ and $Z_b^0(10650)$, respectively. The amplitudes A_{f_0} , A_{f_2} and A_{nr} are the contributions from the $\pi^0\pi^0$ system in an $f_0(980)$, $f_2(1275)$ and a non-resonant state, respectively. Here we assume that the dominant contributions are from amplitudes that preserve the orientation of the spin of the heavy quarkonium state and thus, both pions in the cascade decay $\Upsilon(5S) \rightarrow Z_b^0\pi^0 \rightarrow \Upsilon(nS)\pi^0\pi^0$ are emitted in an S -wave with respect to the heavy quarkonium system. As demonstrated in Ref. [2], angular analysis supports this assumption. Consequently, we parameterize both amplitudes with an S -wave Breit-Wigner function

$$\text{BW}(s, M, \Gamma) = \frac{\sqrt{M\Gamma}}{M^2 - s - iM\Gamma} , \quad (4)$$

where we neglect the possible s dependence of the resonance width. Both amplitudes are symmetrized with respect to π^0 interchange. The masses and widths are fixed to the values obtained in the $\Upsilon(nS)\pi^+\pi^-$ analysis: $M(Z_1) = 10607.2 \text{ MeV}/c^2$, $\Gamma(Z_1) = 18.4 \text{ MeV}/c$, $M(Z_2) = 10652.2 \text{ MeV}/c^2$, $\Gamma(Z_2) = 11.5 \text{ MeV}/c$ [1]. Contributions from the $f_0(980)$ and $f_2(1275)$ are also included in the fit. We use a Flatté function for the $f_0(980)$ and a Breit-Wigner function for the $f_2(1275)$. Coupling constants of the $f_0(980)$ were fixed at values from the $B^+ \rightarrow K^+\pi^+\pi^-$ analysis: $M = 950 \text{ MeV}/c^2$, $g_{\pi\pi} = 0.23$, $g_{KK} = 0.73$ [6]. The mass and width of the $f_2(1275)$ resonance are fixed to the world average values [7]. Following suggestions in Ref. [8], the non-resonant amplitude A_{nr} is parameterized as

$$A_{\text{nr}} = A_{\text{nr}}^1 e^{i\phi_{\text{nr}}^1} + A_{\text{nr}}^2 e^{i\phi_{\text{nr}}^2} s_3 , \quad (5)$$

where A_{nr}^1 , A_{nr}^2 , ϕ_{nr}^1 and ϕ_{nr}^2 are free parameters in the fit. As there is only sensitivity to the relative amplitudes and phases between decay modes, we fix $A_{\text{nr}}^1 = 10.0$ and $\phi_{\text{nr}}^1 = 0.0$.

The logarithmic likelihood function is defined as

$$\mathcal{L} = -2 \sum \log\{\epsilon(s_1, s_2)(f_{\text{sig}}S(s_1, s_2) + (1 - f_{\text{sig}})B(s_1, s_2))\} , \quad (6)$$

where $S(s_1, s_2)$ is $|M(s_1, s_2)|^2$ convoluted with the detector resolution ($6.0 \text{ MeV}/c^2$ for $\Upsilon(nS)\pi^0$ combinations), $\epsilon(s_1, s_2)$ describes the variation of the reconstruction efficiency over the Dalitz plot and f_{sig} is the fraction of signal events in the data sample. The fraction f_{sig} is determined separately for each $\Upsilon(nS)$ decay mode (see Table I). The function $B(s_1, s_2)$ describes the distribution of background events over the phase space. Both products $\epsilon(s_1, s_2) \cdot S(s_1, s_2)$ and $\epsilon(s_1, s_2) \cdot B(s_1, s_2)$ are normalized to unity.

Results from one-dimensional projections of the fits are shown in Figs. 3 and 4. These projections are very similar to the corresponding distributions in $\Upsilon(nS)\pi^+\pi^-$ [1]. A Z_b^0 signal is most clearly seen in $M(\Upsilon\pi^0)_{\max}$. Table II shows the values and errors of amplitudes and phases obtained from the fit to the $\Upsilon(nS)\pi^0\pi^0$ Dalitz plot. The statistical significance of the $Z_b^0(10610)$ signal in the $\Upsilon(2S)\pi^0\pi^0$ sample is 5.3σ . This value is obtained from the

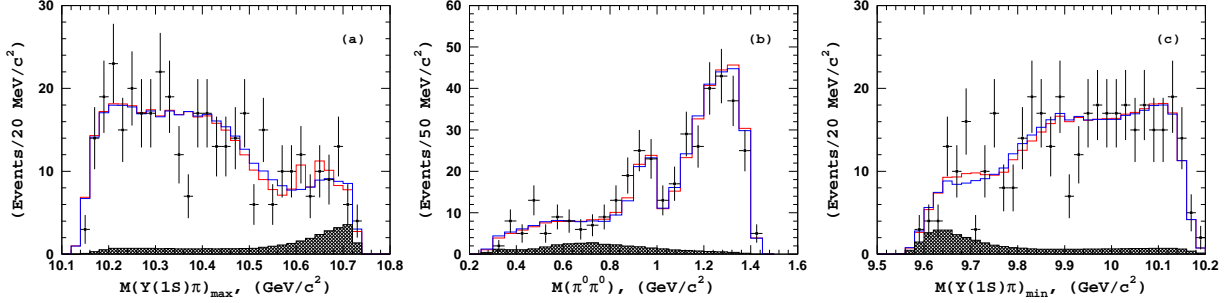


FIG. 3: Comparison of the fit results (open histograms) with experimental data (points with error bars) for $\Upsilon(1S)\pi^0\pi^0$ events in the signal region. Red and blue open histograms show the fit with and without Z_b^0 's, respectively. Hatched histograms show the background components.

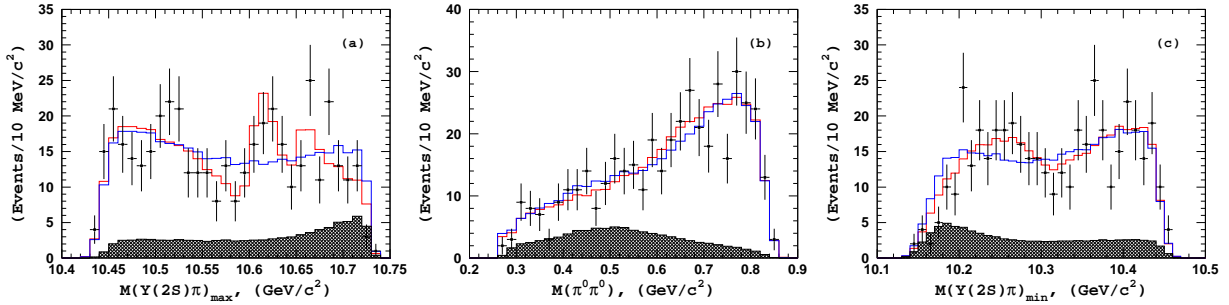


FIG. 4: Comparison of the fit results (open histograms) with experimental data (points with error bars) for $\Upsilon(2S)\pi^0\pi^0$ events in the signal region. Red and blue open histograms show the fit with and without Z_b^0 's, respectively. Hatched histograms show the background components.

TABLE II: Results of the Dalitz plot fit of $\Upsilon(nS)\pi^0\pi^0$ events.

	$\Upsilon(1S)\pi^0\pi^0$	$\Upsilon(1S)\pi^0\pi^0$	$\Upsilon(2S)\pi^0\pi^0$	$\Upsilon(2S)\pi^0\pi^0$	$\Upsilon(2S)\pi^0\pi^0$
Model	with Z_b^0 's	w/o Z_b^0 's	with Z_b^0 's	with Z_1^0 only	w/o Z_b^0 's
$A(Z_1^0)$	$0.50^{+0.34}_{-0.30}$	0.0 (fixed)	$0.58^{+0.21}_{-0.14}$	$0.47^{+0.15}_{-0.11}$	0.0(fixed)
$\phi(Z_1^0)$	-36 ± 50	—	-113 ± 14	-117 ± 17	—
$A(Z_2^0)$	$0.60^{+0.51}_{-0.47}$	0.0 (fixed)	$0.37^{+0.20}_{-0.16}$	0.0 (fixed)	0.0 (fixed)
$\phi(Z_2^0)$	-59 ± 60	—	-125 ± 27	—	—
$A(f_2)$	15.7 ± 2.0	14.6 ± 1.6	18.2 ± 7.3	23.9 ± 7.3	28.2 ± 7.0
$\phi(f_2)$	60 ± 11	51 ± 9	36 ± 21	28 ± 13	28 ± 10
$A(f_0)$	1.07 ± 0.15	0.97 ± 0.12	11.5 ± 1.9	10.5 ± 1.9	8.2 ± 2.1
$\phi(f_0)$	168 ± 11	163 ± 10	211 ± 6	213 ± 7	210 ± 8
A_{nr}^2	15.2 ± 1.2	13.9 ± 0.7	34.7 ± 4.9	31.8 ± 4.3	24.6 ± 4.2
ϕ_{nr}^2	162 ± 4	161 ± 4	80 ± 12	85 ± 13	93 ± 15
$-2\log \mathcal{L}$	-316.7	-312.4	-193.1	-186.6	-154.5

TABLE III: Two solutions found in the Dalitz plot fit of $\Upsilon(2S)\pi^0\pi^0$ events.

Solutions	w/o Z_b^0	w/o Z_b^0	with Z_1^0	with Z_1^0	with Z_b^0 's	with Z_b^0 's
	A	B	A	B	A	B
$A(Z_1^0)$	0.0 (fixed)	0.0 (fixed)	$0.46^{+0.15}_{-0.11}$	$1.35^{+0.64}_{-0.33}$	$0.58^{+0.21}_{-0.14}$	1.42 ± 0.48
$\phi(Z_1^0)$	—	—	-117 ± 14	88 ± 18	-113 ± 14	91 ± 21
$A(Z_2^0)$	0.0 (fixed)	0.0 (fixed)	0.0 (fixed)	0.0 (fixed)	$0.37^{+0.20}_{-0.16}$	0.66 ± 0.40
$\phi(Z_2^0)$	—	—	—	—	-125 ± 27	124 ± 37
$A(f_2)$	28.2 ± 7.0	41.8 ± 9.0	23.9 ± 7.3	48.7 ± 15.4	18.2 ± 7.3	43.3 ± 15.6
$\phi(f_2)$	28 ± 10	-1 ± 14	18 ± 13	10 ± 16	36 ± 21	132 ± 19
$A(f_0)$	8.2 ± 2.1	13.3 ± 3.6	10.5 ± 1.9	13.4 ± 4.2	11.5 ± 1.9	12.6 ± 4.9
$\phi(f_0)$	210 ± 8	131 ± 11	213 ± 7	134 ± 15	211 ± 6	132 ± 19
A_{nr}^2	24.6 ± 4.2	44.2 ± 10.1	31.8 ± 4.3	50.4 ± 12.2	34.7 ± 4.9	50.8 ± 13.7
ϕ_{nr}^2	93 ± 15	-70 ± 16	85 ± 13	-69 ± 22	80 ± 12	-72 ± 25
$-2\log \mathcal{L}$	-154.5	-155.4	-186.6	-186.3	-193.1	-191.2

p-value, $\Delta(-2\log \mathcal{L})$, with two degrees of freedom, i.e. $\Delta(-2\log \mathcal{L}) = 2\log \mathcal{L}(\text{w/o } Z_b^0) - 2\log \mathcal{L}(10610)$. We also perform a fit with the $Z_b^0(10610)$ mass as a free parameter. The fit with both Z_b^0 's gives $M(Z_b^0(10610)) = 10609^{+8}_{-6} \text{ MeV}/c^2$. A similar value, $10603 \pm 6 \text{ MeV}/c^2$, is obtained in a fit in which only the $Z_b^0(10610)$ is included. The signal for the $Z_b^0(10610)$ is not significant in the fit to the $\Upsilon(1S)\pi^0\pi^0$ events due to the smaller relative branching fraction. The signal for the $Z_b^0(10650)$ is not significant in either $\Upsilon(1, 2S)\pi^0\pi^0$ dataset. Our data do not contradict the existence of $Z_b^0(10650)$, but the available statistics is not enough for the observation of this state.

We search for multiple solutions by doing one thousand fits with randomly assigned amplitudes and phases taken from a model without Z_b^0 contributions. We find an additional solution in the $\Upsilon(2S)\pi^0\pi^0$ final state and no other solutions in $\Upsilon(1S)\pi^0\pi^0$. Table III shows the values and errors of amplitudes and phases obtained for both solutions. The second solution is referred to ‘‘Solution B’’. The $Z_b^0(10610)$ significance in Solution B is 5.3σ , almost the same as in Solution A (the baseline fit).

STUDY OF SYSTEMATIC UNCERTAINTIES IN DALITZ ANALYSIS

Experimental errors may arise from the uncertainty in parameterization of the background PDF. We determine this uncertainty by varying parameters of the background PDF. We use different sideband sub-samples to determine PDF parameters: the low-mass sideband only, or the high-mass sideband, or $\Upsilon(nS) \rightarrow e^+e^-$ events only, or $\Upsilon(nS) \rightarrow \mu^+\mu^-$ events only. The statistical significance of the $Z_b^0(10610)$ in all fits is greater than 4.9σ . Another source of systematic uncertainty is the determination of signal efficiency. To estimate this effect we perform two additional fits with a modified efficiency function: $\sqrt{\epsilon(s_{\text{max}}, s_3)}$ and $\epsilon^{3/2}(s_{\text{max}}, s_3)$. The result, $\Delta(-2\log \mathcal{L})$ for models with $Z_b^0(10610)$ and without Z_b^0 's changes from 32.1 to 32.9 and 31.2, respectively. the difference in $Z_b^0(10610)$ significance is less than 0.1. We also perform a fit with a modified detector resolution function: the resolutions are varied from 4 to 8 MeV/ c^2 instead of the nominal 6 MeV/ c^2 to take into account the effect

of different momentum resolutions in MC and data. The resulting changes in $\Delta(-2\log\mathcal{L})$ are less than 0.5 (difference in $Z_b^0(10610)$ significance is less than 0.05).

The model uncertainty originates mainly due to the parameterization of the non-resonant amplitude. To estimate it we vary the model used to fit the data. Three additional models, based on solution A, are used: with an additional $\sigma(600)$ resonance, parameterized by a Breit-Wigner function with $M = 600 \text{ MeV}/c^2$ and $\Gamma = 400 \text{ MeV}/c$, a model with $A_{\text{nr}} = ae^{i\phi_a} + be^{i\phi_b}\sqrt{s(\pi^0\pi^0)}$, and a model without any $f_0(980)$ contribution (to fit $\Upsilon(2S)\pi^0\pi^0$ events only). The smallest $Z_b^0(10610)$ significance is obtained in the last model: 4.9σ . We use this value as the final $Z_b^0(10610)$ significance. Fits with the $Z_b^0(10610)$ mass as a free parameters give values from 10603 to 10615 MeV/c^2 . We use $\pm 6 \text{ MeV}/c^2$ as a model uncertainty for the $Z_b^0(10610)$ mass.

CONCLUSION

We report the observation of $\Upsilon(5S) \rightarrow \Upsilon(1, 2S)\pi^0\pi^0$ decays. The measured branching fractions, $\mathcal{B}(\Upsilon(5S) \rightarrow \Upsilon(1S)\pi^0\pi^0) = (2.25 \pm 0.11 \pm 0.20) \times 10^{-3}$, $\mathcal{B}(\Upsilon(5S) \rightarrow \Upsilon(2S)\pi^0\pi^0) = (3.66 \pm 0.22 \pm 0.48) \times 10^{-3}$, are found to be consistent with the expectation from isospin, scaling from $\mathcal{B}(\Upsilon(5S) \rightarrow \Upsilon(nS)\pi^+\pi^-)$ [9].

Evidence of a neutral resonance decaying to $\Upsilon(2S)\pi^0$, $Z_b^0(10610)$, has been obtained in a Dalitz plot analysis of $\Upsilon(5S) \rightarrow \Upsilon(2S)\pi^0\pi^0$ decay. The statistical significance of the $Z_b^0(10610)$ signal is 5.3σ (4.9σ including model and systematic uncertainties). Its measured mass, $M(Z_b^0(10610)) = 10609_{-6}^{+8} \pm 6 \text{ MeV}/c^2$, is consistent with the mass of the corresponding charged state, the $Z_b^\pm(10610)$. The $Z_b^0(10650)$ signal is not significant in either $\Upsilon(1S)\pi^0\pi^0$ or $\Upsilon(2S)\pi^0\pi^0$. Our data do not contradict the existence of $Z_b^0(10650)$, but the available statistics is not enough for the observation of this state.

ACKNOWLEDGMENTS

We thank the KEKB group for the excellent operation of the accelerator; the KEK cryogenics group for the efficient operation of the solenoid; and the KEK computer group, the National Institute of Informatics, and the PNNL/EMSL computing group for valuable computing and SINET4 network support. We acknowledge support from the Ministry of Education, Culture, Sports, Science, and Technology (MEXT) of Japan, the Japan Society for the Promotion of Science (JSPS), and the Tau-Lepton Physics Research Center of Nagoya University; the Australian Research Council and the Australian Department of Industry, Innovation, Science and Research; the National Natural Science Foundation of China under contract No. 10575109, 10775142, 10875115 and 10825524; the Ministry of Education, Youth and Sports of the Czech Republic under contract No. LA10033 and MSM0021620859; the Department of Science and Technology of India; the Istituto Nazionale di Fisica Nucleare of Italy; the BK21 and WCU program of the Ministry Education Science and Technology, National Research Foundation of Korea, and GSDC of the Korea Institute of Science and Technology Information; the Polish Ministry of Science and Higher Education; the Ministry of Education and Science of the Russian Federation and the Russian Federal Agency for Atomic Energy; the Slovenian Research Agency; the Swiss National Science Foundation; the National Science Council and the Ministry of Education of Taiwan; and the U.S. Department of Energy and the National Science Foundation. This work is supported by a Grant-in-Aid

from MEXT for Science Research in a Priority Area (“New Development of Flavor Physics”), and from JSPS for Creative Scientific Research (“Evolution of Tau-lepton Physics”).

- [1] A. Bondar, A. Garmash, R. Mizuk, D. Santel, K. Kinoshita, et al. (Belle Collaboration) Phys. Rev. Lett. 108, 122001 (2012).
- [2] I. Adachi et al. (Belle Collaboration), arXiv:1105.4583.
- [3] A.E. Bondar, A. Garmash, A.I. Milstein, R. Mizuk, M.B. Voloshin, Phys. Rev. D 84, 054010 (2011).
- [4] A. Abashian et al. (Belle Collaboration), Nucl. Instrum. Methods Phys. Res., Sect. A 479, 117 (2002).
- [5] S. Kurokawa and E. Kikutani, Nucl. Instrum. Methods Phys. Res. Sect. A 499, 1 (2003), and other papers included in this Volume.
- [6] A. Garmash et al. (Belle Collaboration), Phys.Rev.Lett. 96, 251803 (2006).
- [7] J. Beringer et al. (Particle Data Group), Phys. Rev. D86, 010001 (2012).
- [8] M.B. Voloshin, Prog. Part. Nucl. Phys. 61, 455 (2008). M.B. Voloshin, Phys. Rev. D 74, 054022 (2006) and references therein.
- [9] K.-F. Chen, W.-S. Hou, M. Shapkin, A. Sokolov et al. (The Belle collaboration) Phys. Rev. Lett. 100 112001 (2008).